Title

Lymphocyte Invasion in IC10/Basal-Like Breast Tumors Is Associated with Wild-Type TP53

Permalink

https://escholarship.org/uc/item/6z9057ds

Authors

Quigley, David
Silwal-Pandit, Laxmi
Dannenfelser, Ruth
et al.

Peer reviewed

Lymphocyte invasion in IC10/Basal-like breast tumors is associated with wild-type *TP53*

David Quigley[1,2,3], **Laxmi Silwal-Pandit**[1,2], **Ruth Dannenfelser**[4,5], **Anita Langerød**[1,2], **Hans Kristian Moen Vollan**[1,2,6], **Charles Vaske**[7], **Josie Ursini Siegel**[8], **Olga Troyanskaya**[4,5], **Suet-Feung Chin**[9], **Carlos Caldas**[9,10,11], **Allan Balmain**[3], **Anne-Lise Børresen-Dale**[1,2], and **Vessela Kristensen**[1,2,12]

[1]Department of Genetics, Institute for Cancer Research, Oslo University Hospital, The Norwegian Radium Hospital, Oslo, 0310, Norway

[2]K.G. Jebsen Centre for Breast Cancer Research, Institute for Clinical Medicine, Faculty of Medicine, University of Oslo, Oslo, 0313, Norway

[3]Helen Diller Family Comprehensive Cancer Center, University of California at San Francisco, San Francisco, California, 94158 USA

[4]Department of Computer Science, Princeton University, Princeton NJ 08544, USA

[5]Lewis-Sigler Institute for Integrative Genomics, Princeton University, Princeton, NJ 08540, USA

[6]Department of Oncology, Oslo University Hospital, the Norwegian Radium Hospital, 0310, Norway

[7]Five3 Genomics, Inc. Santa Cruz, CA 95060, USA

[8]Lady Davis Institute for Medical Research, Montreal, QC, H3T 1E2, Canada

[9]Cancer Research UK, Cambridge Institute and Department of Oncology, University of Cambridge, Cambridge CB2 0RE, UK

[10]Cambridge Breast Unit, Addenbrooke's Hospital, Cambridge University Hospital NHS Foundation Trust and NIHR Cambridge Biomedical Research Centre, Cambridge CB2 2QQ, UK

[11]Cambridge Experimental Cancer Medicine Centre, Cambridge CB2 0RE, UK

[12]Department of Clinical Molecular Oncology, Division of Medicine, Akershus University Hospital, 1478 Ahus, Norway

Abstract

Lymphocytic infiltration is associated with better prognosis in several epithelial malignancies including breast cancer. The tumor suppressor TP53 is mutated in approximately 30% of breast adenocarcinomas, with varying frequency across molecular subtypes. In this study of 1,420 breast tumors, we tested for interaction between *TP53* mutation status and tumor subtype determined by

Correspondence to: Anne-Lise Børresen-Dale; Vessela Kristensen.

PAM50 and Integrative Cluster analysis. In Integrative Cluster 10 (IC10)/Basal-like breast cancer we identify an association between lymphocytic infiltration, determined by an expression score, and retention of wild-type *TP53*. The expression-derived score agreed with the degree of lymphocytic infiltration assessed by pathological review, and application of the Nanodissect algorithm was suggestive of this infiltration being primarily of cytotoxic T lymphocytes (CTL). Elevated expression of this CTL signature was associated with longer survival in IC10/Basal-like tumors. These findings identify a new link between the TP53 pathway and the adaptive immune response in ER-negative breast tumors, suggesting a connection between TP53 inactivation and failure of tumor immunosurveillance.

IMPLICATIONS—The association of lymphocytic invasion of estrogen receptor-negative breast tumors with the retention of wild-type *TP53* implies a novel protective connection between TP53 function and tumor immunosurveillance.

INTRODUCTION

TP53 mutations occur in nearly 30% of breast cancers and are associated with worse survival and response to doxorubicin therapy (1–4). Breast cancer has been divided at the molecular level into five intrinsic subtypes (Luminal A, Luminal B, HER2-enriched, Normal-like and Basal-like) using mRNA expression (5,6), and a 50 gene classifier has been developed and is widely used (7). Additional subclassifications using miRNA expression and DNA methylation levels have also been proposed (8,9). The METABRIC study further refined our understanding of breast cancer heterogeneity, identifying 10 integrative clusters (IC) by combining mRNA expression with DNA copy number alterations (10). None of these subtype definitions make use of the patient's *TP53* mutation status. *TP53* mutation is more frequent in ER-negative tumors, with highest frequency in the IC10/Basal-like subtypes. In patients with Luminal B, HER2-enriched, or Normal-like tumors *TP53* mutations confer worse survival (3), but no robust association between loss of wild-type *TP53* and survival in IC10/Basal-like tumors has been reported (1,3,11). This suggests that additional factors modulate the effect of *TP53* on survival in these particular cancers.

It is now generally accepted that the adaptive immune system can recognize some tumors and halt their spread or even eliminate them (12) (reviewed in (13–15)). Organ transplant patients with compromised immune systems have an elevated risk of developing certain malignancies, particularly non-melanoma skin cancer (16,17). When functioning properly, the adaptive immune system identifies damaged or infected cells and kills them using granzyme and perforin delivered by cytotoxic T lymphocytes (CTLs). The immunosurveillance model suggests that tumors persist by evading immune recognition. Efforts to harness the immune system to eradicate tumors are the subject of intense research (18).

A metric measuring the number and location of CD8$^+$ and CD45RO$^+$ T cells invading epithelial tumors (the Immunoscore) has recently been proposed as a prognostic marker (19). The presence of CD8+ cytotoxic T cells in ER-negative and ER-positive/HER2-positive breast tumors is associated with significant reductions in relative risk of death from disease (20–26). We recently reported that breast tumors with a higher ratio of T_H1- to T_H2-

associated pathway activity had better outcome (21,27). It is not known why immune cells infiltrate some tumors and not others. Here we demonstrate an association between retention of wild-type *TP53* (*TP53*-WT) alleles and increased infiltration of CTL in ER-negative tumors but not ER-positive tumors, linking these two phenomena and suggesting a subtype-specific link between TP53 function and immunosurveillance.

MATERIALS AND METHODS

Data acquisition

Microarray measurements of tumor mRNA expression and DNA copy number from the METABRIC study were obtained from the European Genome-phenome archive (accession EGAS00000000083) and from GEO accession GSE3494. Illumina Human WG version 3 probe annotations were downloaded from the ReMOAT Illumina annotation (28) (http://compbio.sysbiol.cam.ac.uk/Resources/Annotation). We determined 26,915 probes to be expressed above background levels. *TP53* sequence was assessed by manual review of Sanger sequencing results as described in (3), with 1,420 tumors successfully assessed for mutation status. Tumor infiltration scores were published by Silwal-Pandit and colleagues (3). Tumors were assessed by review of Hematoxylin and Eosin stained tissue sections by a pathologist. Tumors with scattered, discrete lymphocytes were scored as mild, and tumors with confluent sheets of lymphocytes were scored as severe. *TP53* loss of heterozygosity was scored by assessing DNA copy number at the *TP53* locus using the ASCAT algorithm (29). Both gene expression and *TP53* mutation status were available for 1,420 tumors. All of infiltration score, *TP53* mutation status and gene expression data resulting in a successful PAM50 tumor subtype call were available for 1,086 tumors.

Statistical analysis

Statistical calculations were performed in R (30). Interaction between *TP53* status and PAM50 assignment was tested by analysis of variance (ANOVA) in the Discovery and Validation cohorts separately. Interaction in the METABRIC data was considered significant if $P_{interaction}$ 0.05 after multiple testing correction by Holm's adjustment for 26,915 tests. ANOVA models were assessed by visual inspection of Q-Q plots and of plots comparing residual *vs.* fitted values. We obtained non-parametric P values for ANOVA results by testing the interaction between *TP53* status and PAM50 assignment in 1000 permutations of the sample ordering for each probe while maintaining the original *TP53* and tumor subtype factor ordering (31,32). Non-parametric P values for each probe were derived from the rank of the observed parametric P value in a sorted list of P values from permuted data for that probe. Linear models in the Miller dataset were constructed as for METABRIC, but with ER status rather than PAM50 subtype as the parameter interacting with *TP53* mutation status. Results in the Miller dataset were considered statistically significant if $P_{interaction} < 0.05$ after multiple testing correction by Holm's adjustment for 103 tests.

Survival analysis log rank tests were considered significant at $P < 0.05$. Gene Ontology enrichment analysis was performed using the BiNGO package (33). Pathway enrichment was tested using QuSAGE, a gene set enrichment test that produces probability distributions for enrichment scores and corrects for correlation between genes within a gene set (34). The

False Discovery Rate values for QuSAGE were calculated using the Benjamini-Hochberg as implemented by the *p. adjust* function in R. Individual CTL, T_H1, and T_H2 scores for each tumor were generated by calculating the standardized expression for genes on each list and taking the mean of those values.

Gene pathway analysis

Gene lists derived from flow-cytometry separation of lymphocytes were obtained from results published in (35). Nanodissection was performed as described in (36); briefly, Nanodissect uses a support vector machine within an iterative framework to handle standards of varying specificity. To derive gene lists, this method was applied on a diverse compendium of human microarray data with hand-curated immune markers for CTL, T_H1, and T_H2 cells. Each of the 69,708 samples in the compendium was processed from CEL files using RMA background correction, quantile normalization, and median polish. A cut-off was applied to the resulting gene lists restricting them to the top 150 most likely genes. Genes appearing in multiple lists were randomly assigned to one list and removed from the others.

RESULTS

Basal-like *TP53*-WT tumors preferentially expressed cytotoxic T cell markers

We analyzed gene expression and *TP53* mutation status in the METABRIC cohort of breast cancer patients, data previously reported in (3,10). The METABRIC cohort consists of separate Discovery and Validation subsets. We obtained both *TP53* mutation status and gene expression microarray results for 803 and 617 patients in the Discovery and Validation sets, identifying 218 and 176 *TP53*-mutant tumors respectively. ER-negative tumors were significantly more likely to harbor a *TP53* mutation than ER-positive tumors (P < 0.001, Fisher's exact test, Table 1). Because *TP53* mutation is associated with worse survival in Luminal B, Normal-like, and HER2-enriched tumors but not Basal-like tumors (3), we hypothesized that alterations in TP53 function due to *TP53* mutation would have distinct effects on gene expression in the different intrinsic subtypes. Such differences might help explain the apparent absence of association between *TP53* mutation and survival in Basal-like tumors.

We therefore constructed a linear model for expression of each gene that included three terms: *TP53* mutation status, PAM50 subtype, and the interaction between these terms (see Materials and Methods). We identified 219 probes with significant interactions in the Discovery cohort and 548 probes in the Validation cohort. These lists had 124 probes in common, comprising 103 genes (listed in supplementary Table 1). A larger percentage of the tumors in the Validation cohort with known *TP53* mutation status were Basal-like (22% in the Validation cohort vs. 12% in the Discovery cohort), which may explain why more significant interactions were identified in this cohort.

For some probes, residual values were not normally distributed or had heteroscedastic variance between strata, conditions which would violate the assumptions of the ANOVA (Materials and Methods). To test whether our findings were robust to these issues we

performed a non-parametric permutation analysis of interaction significance for the Discovery and Validation sets (see Materials and Methods). Probesets with the strongest P value for interaction in the parametric ANOVA also had the most significant P value for interaction as assessed by permutation analysis (supplementary Fig. 1). We found 358 probes (314 genes) to be significant at P < 0.001 in both cohorts using the permutation approach, including all but one of the 103 genes identified by the parametric approach (*TESPA1*), supporting our finding that interaction between *TP53* mutation status and tumor subtype was statistically significant for these genes.

The main effect identified in both cohorts by this analysis was upregulation of immune-related genes in the Basal-like *TP53*-WT subgroup, as compared to *TP53*-mutant tumors (Fig. 1a). Genes with significant interactions between subtype and *TP53* mutation status usually had strongly correlated expression (median Spearman rho=0.64), and pathway analysis by Gene Ontology enrichment testing showed that this gene list was significantly enriched for genes with roles in regulation of T cell activation, T cell receptor signaling and T cell costimulation (corrected $P < 2 \times 10^{-12}$). These included T cell surface antigens (e.g. *CD2*, *CD3D*, *CD4*, *CD6, LY9*), effector molecules for cytotoxic T cells (e.g. perforin), genes important to the T cell antigen receptor pathway (e.g. *CD247*, *ZAP70*), and *CXCR3*, a chemokine receptor participating in tissue infiltration by T cells (37) (Fig. 1b).

We next confirmed the association between elevated expression of T cell markers and *TP53* mutation status in ER-negative tumors in an independent, previously published cohort of 247 breast tumors (38). This cohort was smaller than METABRIC, reducing the statistical power to identify interactions. Although the mean difference in T cell gene expression levels between ER-negative *TP53*-WT and *TP53*-mutant tumors was also smaller than what we observed in the METABRIC data, we confirmed significant interaction for fourteen of the 103 genes identified in the METABRIC analysis, including *CXCR3*, *CD2*, *CD3E*, *LY9*, and *IL2RG* ($P_{interaction} < 4.9 \times 10^{-4}$, Fig. 1c).

Cytotoxic T cell mRNA expression correlated with lymphocytic infiltration assessed by histopathology

We assessed the degree to which elevated expression of T cell genes was associated with the presence of immune cells by comparing expression of lymphocytic markers to lymphocytic infiltration scores (graded as absent, mild, or severe, see Materials and Methods). ER-negative tumors had significantly higher degrees of infiltration than ER-positive tumors (P < 0.001, Chi-squared test for trend) with the highest percentage of severe infiltration occurring in Basal-like tumors (Table 1). Across all tumor subtypes, lymphocytic infiltration determined by histopathology was strongly correlated with expression of *CD2*, *CD3E*, *CCR7*, and other genes associated with lymphocytes (Fig. 2a).

CTL and T$_H$1 expression scores were higher in ER-negative and IC10/Basal-like *TP53*-WT tumors than *TP53*-mutant tumors

For subsequent analysis we calculated expression scores for CTL, T$_H$1, and T$_H$2 genes using two complementary approaches. We first generated CTL, T$_H$1, and T$_H$2 gene lists using Nanodissect, an *in silico* method to identify genes with cell-lineage specific expression (36)

(gene lists in supplementary Tables 2 and 3). The correlation between increases in lymphocyte infiltration assessed by histopathology and increased CTL score was strong (Fig. 2b). CTL score was correlated positively with T_H1 score ($r^2 = 0.49$, $P < 0.001$) and inversely with T_H2 expression score ($r^2 = 0.17$, $P < 0.001$). We identified a significant interaction between TP53 mutation status and tumor subtype associated with CTL score using the parametric ANOVA model ($P = 3 \times 10^{-17}$). The lowest P value in 100,000 random sample permutations using this model was 4.8×10^{-6}, supporting our finding that the interaction between *TP53* mutation status and tumor subtype was statistically significant for the CTL score. We obtained similar results using gene lists derived from gene expression microarray analysis of cell fractions obtained by flow-cytometry separation of lymphocytes (35) (supplementary Fig. 2).

We then compared these scores in *TP53*-WT and *TP53*-mutant tumors by pathway differential expression analysis (34). ER-positive *TP53* mutant tumors had slightly lower T_H1 scores, while ER-negative *TP53* wild-type tumors had significantly higher CTL scores and lower T_H2 scores (Fig. 3a). Within the intrinsic subtypes, no score was significantly different in Luminal A or Normal-like tumors, while *TP53*-mutant Luminal B tumors had lower CTL and T_H1 scores (Fig. 3b). *TP53*-mutant HER2-enriched tumors had slightly lower T_H2 scores, while *TP53*-mutant Basal-like tumors had higher CTL scores and lower T_H2 scores (Fig. 3b). Within the Integrative Clusters, IC4 and IC10 had clearly higher CTL scores compared to other subtypes. IC4, which is enriched for tumors with heavy lymphocytic infiltration, on the basis of copy number analysis (showing the deletions corresponding to T-cell receptor rearrangement), gene expression and histological assessment, had the highest CTL score (Table 2, Supplementary Fig. 3). But, whereas IC10 tumors (which are Basal-like tumors with genomic instability) that were *TP53*-WT had higher CTL and T_H1 scores and lower T_H2 scores, IC4 tumors (which have mostly flat genomic profiles) had no significant difference in CTL/T_H1/T_H2 scores related to *TP53* mutation status (Fig. 3c).

Both *TP53* mutation and loss of heterozygosity correlated with CTL scores in IC10/Basal-like tumors

There is evidence from biochemical analysis *in vitro* and *in vivo* that while many *TP53* missense mutations result in loss of function or exert dominant negative effects, some result in gain of function (reviewed in (39)). Truncating mutations in *TP53* (e.g. premature stop codons), which inactivate the protein, were more frequent in Basal-like and HER2-enriched tumors (3). Nevertheless, after adjusting for subtype, we did not identify a significant correlation between immune scores and *TP53* mutation type (data not shown).

If *TP53* loss of heterozygosity (*TP53*-LOH) could phenocopy *TP53* mutation, we would expect *TP53*-LOH would also be associated with lower CTL scores. To test this we fitted a linear model for CTL score using *TP53*-LOH status, *TP53*-mutation status, and the interaction between *TP53*-LOH and *TP53*-mutation status as terms. *TP53*-WT tumors with copy-number neutral LOH were counted as *TP53*-LOH[+], as these tumors had lower expression of *TP53* mRNA than *TP53*-WT tumors without LOH (Supplementary Fig. 4).

In ER-negative, Basal-like, and IC10 tumors, both *TP53* mutation and *TP53*-LOH were associated with lower CTL scores when evaluated as a single factor (P < 0.001) and after adjusting for the effect of the other factor (P < 0.05, Fig. 4a–c). Neither factor was significant in ER-positive tumors or Normal-like tumors. After stratifying HER2-enriched tumors by ER status, both *TP53* mutation and *TP53*-LOH were significantly and independently associated with CTL score in ER-negative but not ER-positive tumors (P < 0.05, Supplementary Fig. 5). In IC4 tumors *TP53*-LOH but not *TP53*-mutation status was associated with lower CTL score (P < 0.05, Fig. 4d). We did not find evidence for a statistical interaction between these two factors in any subgroup. In cases where both associations were significant, the decrease in CTL score associated with *TP53*-LOH was larger than that associated with *TP53* mutation (Fig 4a–c).

Elevated CTL expression score was associated with better survival in IC10/Basal-like tumors

Several previous reports have found an association between elevated expression of immune cell genes and/or lymphocytic infiltration and better survival in Basal-like or ER-negative tumors (20,22–26). We divided samples into four quartiles by their CTL scores and compared survival of patients in the highest quartile (the highest CTL scores) to those in the other three quartiles (Materials and Methods). In a univariate survival analysis, we found a significant association between higher CTL score and longer disease-specific survival in ER-negative (P = 0.001, odds ratio=0.61, C.I. 0.45 to 0.82, log rank test, Fig. 5a), but not ER-positive tumors (Fig. 5b). We found a similar result for Basal-like tumors (P = 0.005, odds ratio = 0.59, C.I. 0.41 to 0.86, log rank test, Fig. 5c) but not HER2-enriched tumors (Fig. 5d). The effect was statistically strongest in IC10 tumors (P = 4×10^{-5}, odds ratio = 0.35, C.I. 0.20 to 0.60, log rank test, Fig. 5e) and not significant in IC4 (Fig. 5f). This effect was significant in ER-negative, Basal-like, and IC10 tumors after correction for the presence of lymph node metastasis, which was the strongest prognostic feature in METABRIC (P < 0.05, log rank test). In contrast, *TP53* status did not provide independent prognostic information in any of these groups in univariate analysis or after adjusting for elevated CTL expression.

DISCUSSION

This study presents association analysis of two independent cohorts supporting a link between TP53 status in breast tumors and CTL expression. The expression-based CTL score, used here as a surrogate of lymphocytic infiltration, was higher in *TP53*-WT vs. mutant ER-negative, Basal-like, and IC10 breast tumors. Women with Basal-like breast tumors and a high CTL score had significantly longer survival. This effect was strongest in the 'core' Basal-like tumors from IC10. The best-understood model for TP53-mediated tumor suppression involves its induction by DNA-damage to induce apoptosis or cell cycle arrest through transcriptional activation of genes controlling these processes (40). TP53 function can be impaired by truncating mutations, missense mutations affecting its DNA-binding motif, somatic loss of one or both copies of a *TP53*-WT allele, or indirect effects such as binding of the TP53 protein to viral proteins or proteins such as MDM2. Our results

suggest that the interaction with *TP53* that we observed was attributable to loss of a *TP53*-WT allele rather than a new *TP53*-mutant-specific function.

Direct evidence for a mechanistic link between TP53 and immunosurveillance will require additional functional studies. It may be that CTL function is influenced by the *TP53* pathway status of tumor cells that are targeted for apoptosis. The primary mechanism for CTL-mediated cell death is induction of apoptosis via the caspase cascade, suggesting that abrogating the TP53 pathway may provide an added benefit to tumor cells in escaping CTL-mediated apoptosis. Studies from the Chouaib lab (41) using a *TP53*-WT melanoma cell line paired with an autologous CTL line have shown evidence for a direct link between *TP53* and CTL function in killing tumor cells. That study showed that granzyme B-mediated tumor cell death was inhibited by knocking down *TP53* expression with siRNA or by treatment with the TP53 inhibitor pifithrin-alpha, and conjugation between CTLs and their targets leads to TP53 protein accumulation (41). These results are compatible with a direct functional link between TP53-mediated apoptosis and CTL function, but independent replication in breast cancer cells is needed to establish whether this model is relevant to Basal-like tumors.

A failure of immunosurveillance to arrest tumor development ("immune escape") can occur by several routes. Some tumors stop producing antigens recognized as foreign by the adaptive immune system. Others deactivate the apoptotic pathways triggered by T cell response. Our data suggest that CTL-mediated immunosurveillance is more effective in ER-negative breast tumors if the tumor still expresses wild-type TP53, and that tumors losing *TP53*-WT alleles gain a selective advantage in part by more successfully evading the adaptive immune system.

Supplementary Material

Refer to Web version on PubMed Central for supplementary material.

Acknowledgments

References

1. Olivier M, Langerød A, Carrieri P, Bergh J, Klaar S, Eyfjord J, et al. The clinical value of somatic TP53 gene mutations in 1,794 patients with breast cancer. Clin Cancer Res. 2006; 12:1157–1167. [PubMed: 16489069]

2. Aas T, Borresen AL, Geisler S, Smith-Sorensen B, Johnsen H, Varhaug JE, et al. Specific P53 mutations are associated with de novo resistance to doxorubicin in breast cancer patients. Nat Med. 1996; 2:811–814. [PubMed: 8673929]

3. Silwal-Pandit L, Moen Vollan HK, Chin SF, Rueda OM, McKinney SE, Osako T, et al. TP53 mutation spectrum in breast cancer is subtype specific and has distinct prognostic relevance. Clin Cancer Res. 2014

4. Bertheau P, Plassa F, Espie M, Turpin E, de Roquancourt A, Marty M, et al. Effect of mutated TP53 on response of advanced breast cancers to high-dose chemotherapy. Lancet. 2002; 360:852–854. [PubMed: 12243922]

5. Perou CM, Sorlie T, Eisen MB, van de Rijn M, Jeffrey SS, Rees CA, et al. Molecular portraits of human breast tumours. Nature. 2000; 406:747–752. [PubMed: 10963602]

6. Sorlie T, Perou CM, Tibshirani R, Aas T, Geisler S, Johnsen H, et al. Gene expression patterns of breast carcinomas distinguish tumor subclasses with clinical implications. Proc Natl Acad Sci U S A. 2001; 98:10869–10874. [PubMed: 11553815]

7. Nielsen TO, Parker JS, Leung S, Voduc D, Ebbert M, Vickery T, et al. A comparison of PAM50 intrinsic subtyping with immunohistochemistry and clinical prognostic factors in tamoxifen-treated estrogen receptor-positive breast cancer. Clin Cancer Res. 2010; 16:5222–5232. [PubMed: 20837693]

8. Enerly E, Steinfeld I, Kleivi K, Leivonen SK, Aure MR, Russnes HG, et al. miRNA-mRNA Integrated Analysis Reveals Roles for miRNAs in Primary Breast Tumors. PLoS ONE. 2011; 6:e16915. [PubMed: 21364938]

9. Ronneberg JA, Fleischer T, Solvang HK, Nordgard SH, Edvardsen H, Potapenko I, et al. Methylation profiling with a panel of cancer related genes: association with estrogen receptor, TP53 mutation status and expression subtypes in sporadic breast cancer. Mol Oncol. 2011; 5:61–76. [PubMed: 21212030]

10. Curtis C, Shah SP, Chin SF, Turashvili G, Rueda OM, Dunning MJ, et al. The genomic and transcriptomic architecture of 2,000 breast tumours reveals novel subgroups. Nature. 2012; 486:346–352. [PubMed: 22522925]

11. Joshi H, Bhanot G, Borresen-Dale AL, Kristensen V. Potential tumorigenic programs associated with TP53 mutation status reveal role of VEGF pathway. Br J Cancer. 2012; 107:1722–1728. [PubMed: 23079576]

12. Galon J, Costes A, Sanchez-Cabo F, Kirilovsky A, Mlecnik B, Lagorce-Pages C, et al. Type, density, and location of immune cells within human colorectal tumors predict clinical outcome. Science. 2006; 313:1960–1964. [PubMed: 17008531]

13. Dunn GP, Bruce AT, Ikeda H, Old LJ, Schreiber RD. Cancer immunoediting: from immunosurveillance to tumor escape. Nat Immunol. 2002; 3:991–998. [PubMed: 12407406]

14. Mantovani A, Romero P, Palucka AK, Marincola FM. Tumour immunity: effector response to tumour and role of the microenvironment. Lancet. 2008; 371:771–783. [PubMed: 18275997]

15. Schreiber RD, Old LJ, Smyth MJ. Cancer immunoediting: integrating immunity's roles in cancer suppression and promotion. Science. 2011; 331:1565–1570. [PubMed: 21436444]

16. Jensen P, Hansen S, Moller B, Leivestad T, Pfeffer P, Geiran O, et al. Skin cancer in kidney and heart transplant recipients and different long-term immunosuppressive therapy regimens. Journal of the American Academy of Dermatology. 1999; 40:177–186. [PubMed: 10025742]

17. Walder BK, Robertson MR, Jeremy D. Skin cancer and immunosuppression. Lancet. 1971; 2:1282–1283. [PubMed: 4143536]

18. Restifo NP, Dudley ME, Rosenberg SA. Adoptive immunotherapy for cancer: harnessing the T cell response. Nat Rev Immunol. 2012; 12:269–281. [PubMed: 22437939]

19. Galon J, Mlecnik B, Bindea G, Angell HK, Berger A, Lagorce C, et al. Towards the introduction of the 'Immunoscore' in the classification of malignant tumours. J Pathol. 2014; 232:199–209. [PubMed: 24122236]

20. Teschendorff AE, Miremadi A, Pinder SE, Ellis IO, Caldas C. An immune response gene expression module identifies a good prognosis subtype in estrogen receptor negative breast cancer. Genome Biol. 2007; 8:R157. [PubMed: 17683518]

21. Teschendorff AE, Gomez S, Arenas A, El-Ashry D, Schmidt M, Gehrmann M, et al. Improved prognostic classification of breast cancer defined by antagonistic activation patterns of immune response pathway modules. BMC Cancer. 2010; 10:604. [PubMed: 21050467]

22. Schmidt M, Bohm D, von Torne C, Steiner E, Puhl A, Pilch H, et al. The humoral immune system has a key prognostic impact in node-negative breast cancer. Cancer Res. 2008; 68:5405–5413. [PubMed: 18593943]

23. Desmedt C, Haibe-Kains B, Wirapati P, Buyse M, Larsimont D, Bontempi G, et al. Biological processes associated with breast cancer clinical outcome depend on the molecular subtypes. Clin Cancer Res. 2008; 14:5158–5165. [PubMed: 18698033]

24. Rody A, Holtrich U, Pusztai L, Liedtke C, Gaetje R, Ruckhaeberle E, et al. T-cell metagene predicts a favorable prognosis in estrogen receptor-negative and HER2-positive breast cancers. Breast Cancer Res. 2009; 11:R15. [PubMed: 19272155]

25. Mahmoud SM, Paish EC, Powe DG, Macmillan RD, Grainge MJ, Lee AH, et al. Tumor-infiltrating CD8+ lymphocytes predict clinical outcome in breast cancer. J Clin Oncol. 2011; 29:1949–1955. [PubMed: 21483002]

26. Ali H, Provenzano E, Dawson S-J, Blows F, Liu BMS, et al. Association between CD8+ T-cell infiltration and breast cancer survival in 12 439 patients. Annals of Oncology. 2014 in press.

27. Kristensen VN, Vaske CJ, Ursini-Siegel J, Van Loo P, Nordgard SH, Sachidanandam R, et al. Integrated molecular profiles of invasive breast tumors and ductal carcinoma in situ (DCIS) reveal differential vascular and interleukin signaling. Proc Natl Acad Sci U S A. 2012; 109:2802–2807. [PubMed: 21908711]

28. Barbosa-Morais NL, Dunning MJ, Samarajiwa SA, Darot JF, Ritchie ME, Lynch AG, et al. A re-annotation pipeline for Illumina BeadArrays: improving the interpretation of gene expression data. Nucleic Acids Res. 2010; 38:e17. [PubMed: 19923232]

29. Van Loo P, Nordgard SH, Lingjaerde OC, Russnes HG, Rye IH, Sun W, et al. Allele-specific copy number analysis of tumors. Proc Natl Acad Sci U S A. 2010; 107:16910–16915. [PubMed: 20837533]

30. R Core Team. R: A Language and Environment for Statistical Computing. 2012.

31. Anderson MJ, Ter Braak CJF. Permutation tests for multi-factorial analysis of variance. J Stat Comput Sim. 2003; 73:85–113.

32. Manly, BFJ. Randomization, bootstrap, and Monte Carlo methods in biology. 3. Chapman & Hall/CRC; 2007.

33. Maere S, Heymans K, Kuiper M. BiNGO: a Cytoscape plugin to assess overrepresentation of gene ontology categories in biological networks. Bioinformatics. 2005; 21:3448–3449. [PubMed: 15972284]

34. Yaari G, Bolen CR, Thakar J, Kleinstein SH. Quantitative set analysis for gene expression: a method to quantify gene set differential expression including gene-gene correlations. Nucleic Acids Res. 2013; 41:e170. [PubMed: 23921631]

35. Gu-Trantien C, Loi S, Garaud S, Equeter C, Libin M, de Wind A, et al. CD4(+) follicular helper T cell infiltration predicts breast cancer survival. J Clin Invest. 2013; 123:2873–2892. [PubMed: 23778140]

36. Ju W, Greene CS, Eichinger F, Nair V, Hodgin JB, Bitzer M, et al. Defining cell-type specificity at the transcriptional level in human disease. Genome Res. 2013; 23:1862–1873. [PubMed: 23950145]

37. Qin S, Rottman JB, Myers P, Kassam N, Weinblatt M, Loetscher M, et al. The chemokine receptors CXCR3 and CCR5 mark subsets of T cells associated with certain inflammatory reactions. J Clin Invest. 1998; 101:746–754. [PubMed: 9466968]

38. Miller LD, Smeds J, George J, Vega VB, Vergara L, Ploner A, et al. An expression signature for p53 status in human breast cancer predicts mutation status, transcriptional effects, and patient survival. Proc Natl Acad Sci U S A. 2005; 102:13550–13555. [PubMed: 16141321]

39. Brosh R, Rotter V. When mutants gain new powers: news from the mutant p53 field. Nat Rev Cancer. 2009; 9:701–713. [PubMed: 19693097]

40. Vousden KH, Prives C. Blinded by the Light: The Growing Complexity of p53. Cell. 2009; 137:413–431. [PubMed: 19410540]

41. Meslin F, Thiery J, Richon C, Jalil A, Chouaib S. Granzyme B-induced cell death involves induction of p53 tumor suppressor gene and its activation in tumor target cells. J Biol Chem. 2007; 282:32991–32999. [PubMed: 17855337]
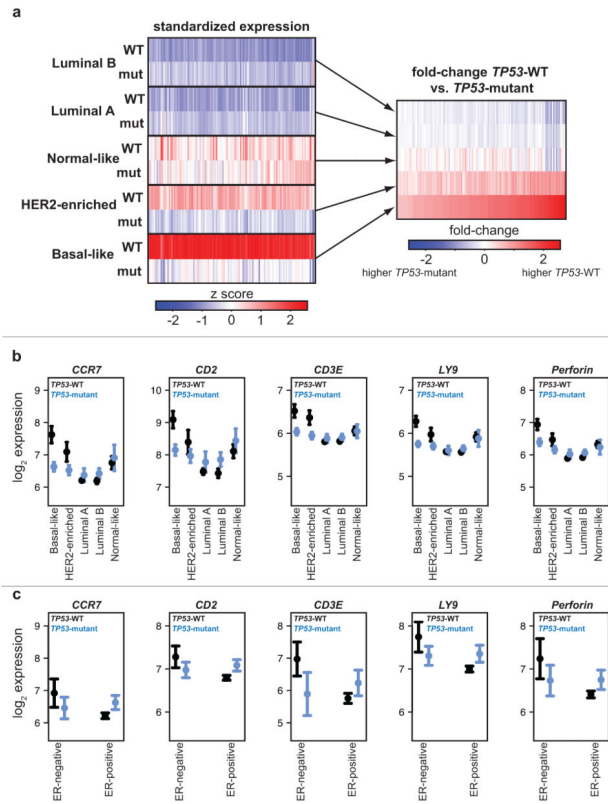
FIGURE 1. *TP53* mutation status is associated with gene expression in Basal-like tumors
(**a**) Heat maps showing standardized expression levels (left) and relative fold-change (right) of 124 probes with significant interaction between *TP53* status and PAM50 subtype in both METABRIC discovery and validation cohorts. *TP53*-WT tumors labeled "WT", *TP53*-mutant tumors labeled "mut". Darker red indicates higher expression and darker blue indicates lower expression. Probes were plotted in the same order, sorted by the magnitude of fold-change in Basal-like tumors (see Supplementary Table 1). (**b**) Effect plots of expression of *CCR7*, *CD2*, *CD3E*, *LY9*, and perforin *(PRF1)* grouped by PAM50 subtype and *TP53* mutation status. *TP53*-WT plotted in black, *TP53*-mutant plotted in blue. Points indicate mean, error bars indicate 95% confidence intervals calculated from twice the standard error. (**c**) Using data from Miller *et al.*, effect plots of expression of *CCR7*, *CD2*, *CD3E*, *LY9*, and perforin *(PRF1)* grouped by ER status and *TP53* mutation status show significant interaction as in the METABRIC data set. Drawn as in Fig. 1B.
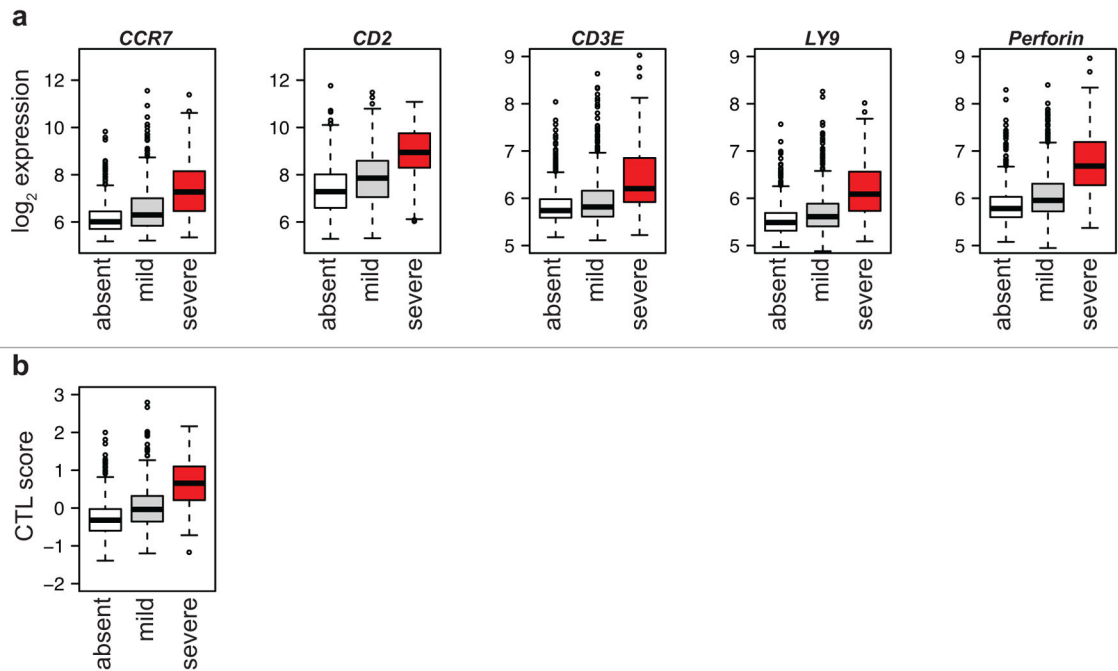
FIGURE 2. Severe immune infiltration was correlated with elevated expression of CTL surface markers

(**a**) Box plots showing expression of *CCR7*, *CD2*, *CD3E*, *LY9*, and *PRF1* increases with increasing severity of pathologically determined lymphocytic infiltration, with a qualitatively higher jump between "mild" and "severe" than between "absent" and "mild".

(**b**) Box plots showing expression of the CTL pathway generated from Nanodissect analysis also increases with increasing severity of pathologically determined lymphocytic infiltration.
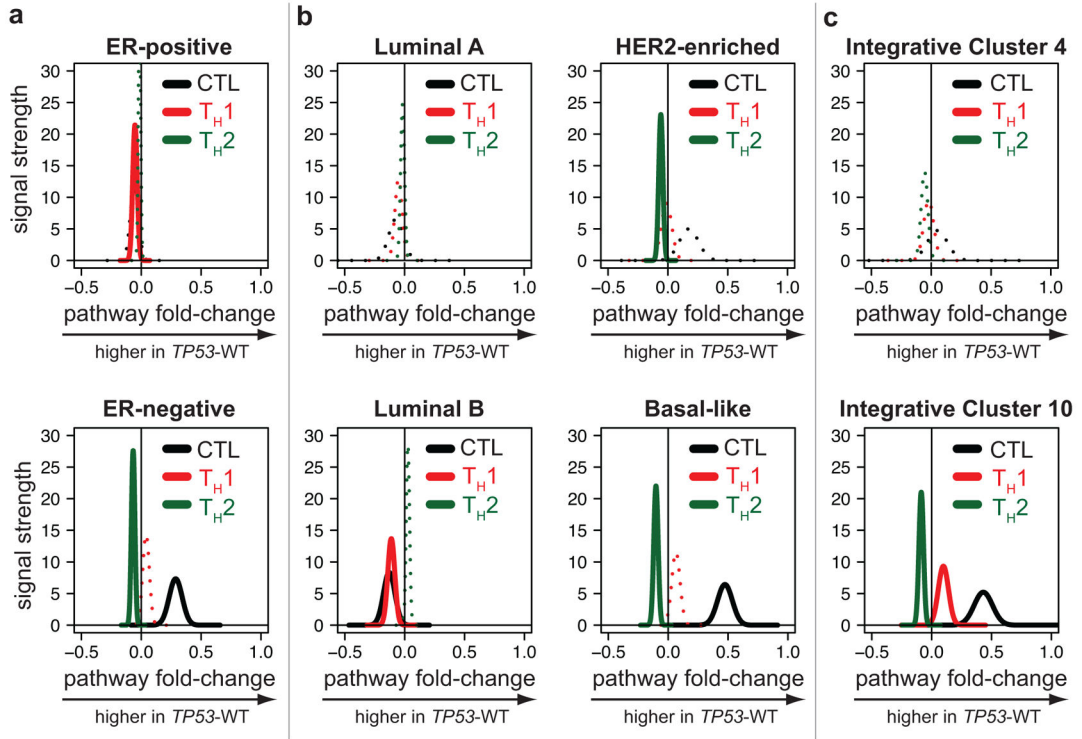
FIGURE 3. Immune infiltrate is enriched for CTL and T_H1 pathways

Plots of estimated fold-change distributions of standardized CTL scores derived from log_2-transformed gene expression measurements comparing *TP53*-WT to *TP53*-mutant tumors separated by (**a**) ER status, (**b**) intrinsic subtype, and (**c**) integrated cluster. Significant differential expression (FDR 0.05) plotted in thick solid lines, non-significant plotted with thin dotted lines. Distribution peaks on the right side of the zero line indicate higher expression in *TP53*-WT tumors. Plots represent a convolution of signal from individual probes in the pathway; for probe lists see supplementary Tables 2 and 3.
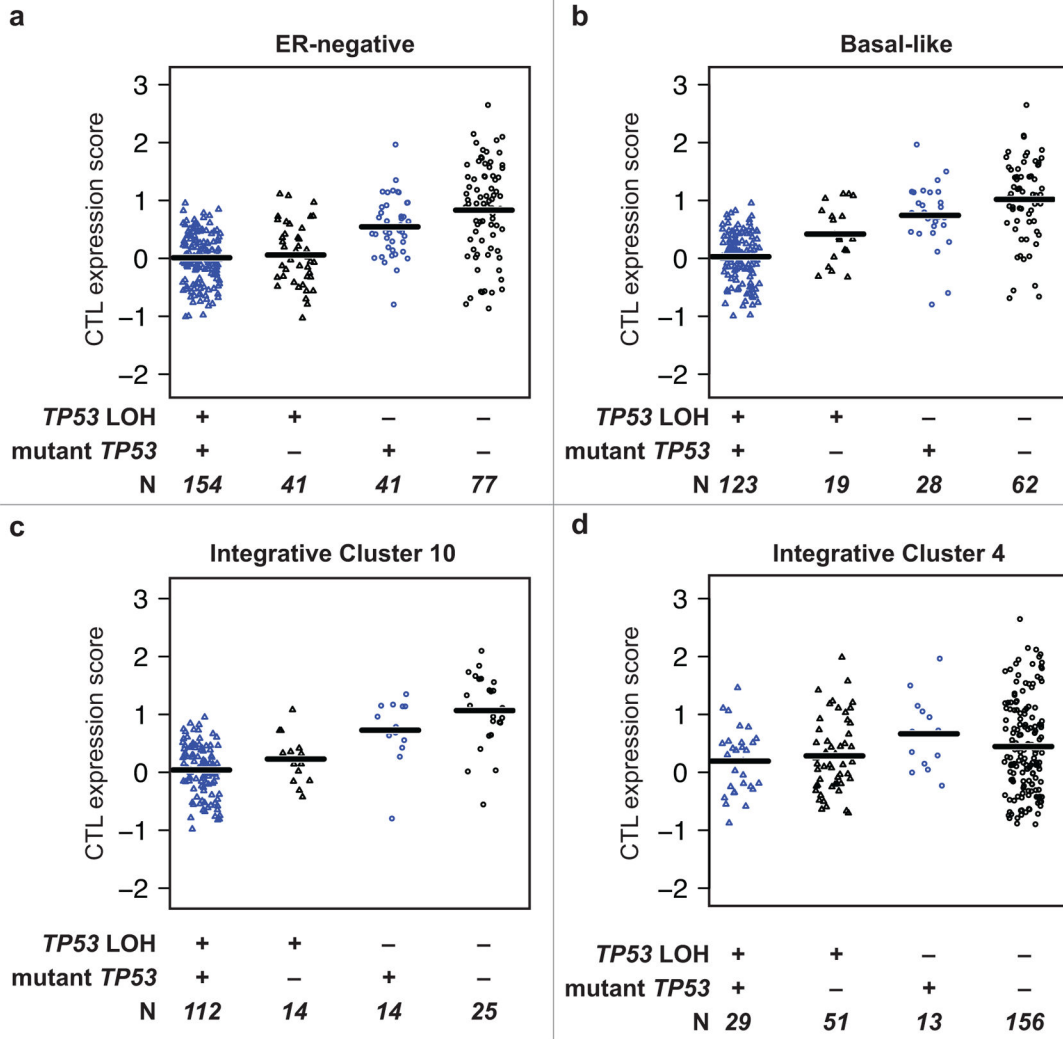
FIGURE 4. Either *TP53*-mutation or *TP53*-LOH is associated with lower expression of the CTL pathway

Plots of CTL pathway expression gene expression divided by *TP53* mutation and LOH status in **(a)** ER-negative, **(b)** Basal-like, **(c)** IC10, and **(d)** IC4 tumors, where + indicates mutation or LOH is present. *TP53*-WT tumors plotted in black, *TP53*-mutant tumors plotted in blue. Tumors without *TP53*-LOH plotted as open circles, tumors with *TP53*-LOH plotted using triangles. Horizontal lines indicate mean expression.
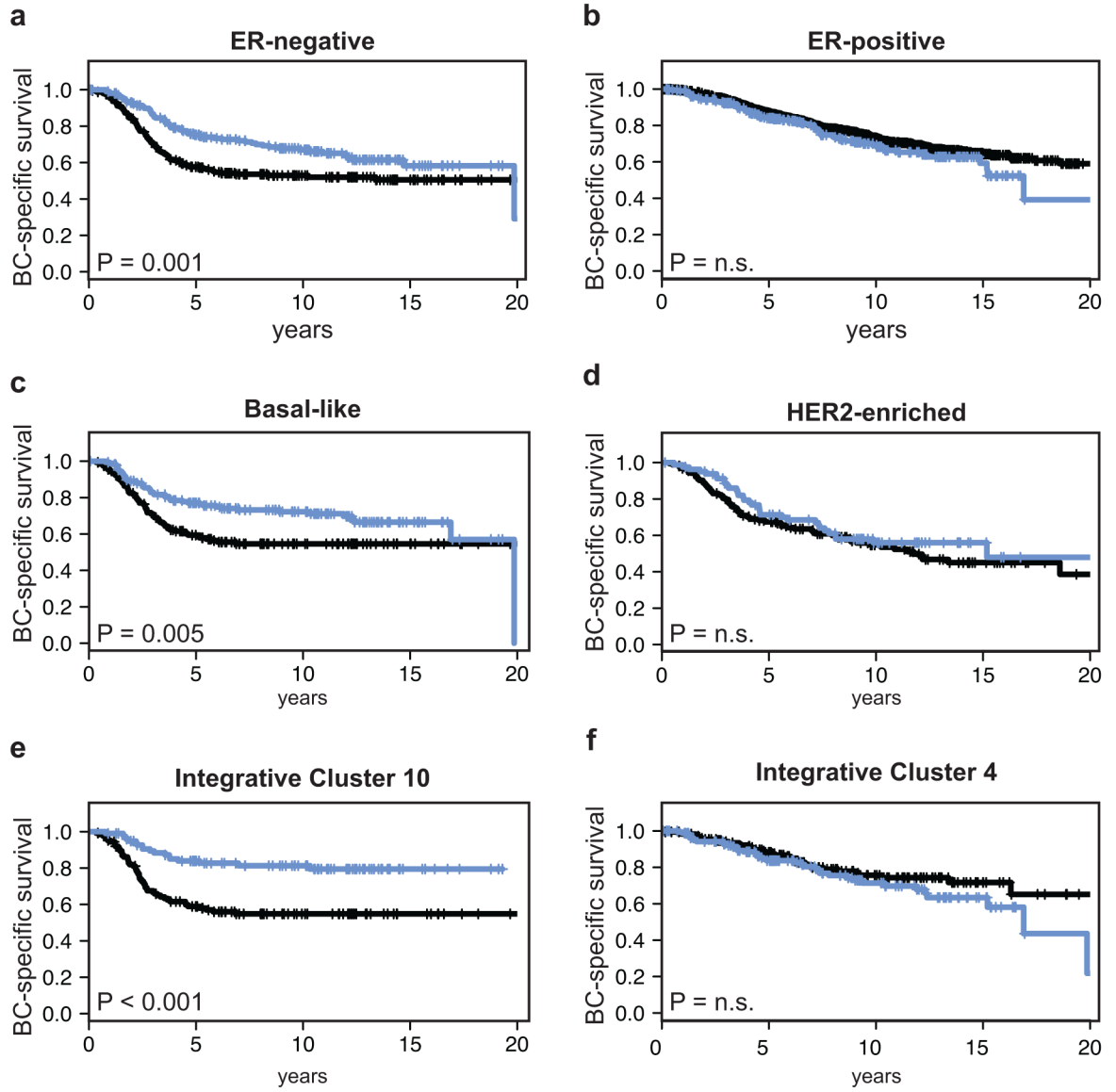
FIGURE 5. elevated CTL expression is associated with better survival in ER-negative tumors
Kaplan-Meier plots comparing breast-cancer-specific survival dividing tumors by those with the highest quartile of CTL expression (blue) or lower CTL expression (black) in **(a)** ER-negative, **(b)** ER-positive, **(c)** Basal-like, **(d)** HER2-enriched, **(e)** IC10, and **(f)** IC4 tumors. Elevated expression of the CTL gene signature was associated with significantly better survival in ER-negative, Basal-like, and IC10 tumors.

Table 1

Summary of *TP53* mutation and lymphocyte infiltration status

	Overall	*TP53* status		Lymphocytic infiltrate			
		WT	Mutant	Absent	Mild	Severe	no call
ER-positive	1101 (78)	906 (82)	195 (18)	324 (37)	471 (54)	75 (09)	231
ER-negative	319 (22)	120 (38)	199 (62)	66 (28)	89 (38)	78 (34)	86
Luminal A	507 (36)	460 (91)	47 (09)	186 (44)	218 (52)	15 (04)	88
Luminal B	379 (27)	285 (75)	94 (25)	105 (35)	156 (52)	39 (13)	79
Normal-like	136 (10)	121 (89)	15 (11)	23 (21)	71 (66)	13 (12)	29
HER2-enriched	161 (11)	75 (47)	86 (53)	37 (33)	46 (41)	29 (26)	49
Basal-like	234 (17)	82 (35)	152 (65)	38 (23)	68 (42)	57 (35)	71
no call	3	3	0	1	1	0	1
IC1	107 (08)	83 (78)	24 (22)	31 (36)	43 (49)	13 (15)	20
IC2	54 (04)	43 (80)	11 (20)	20 (42)	22 (46)	6 (12)	6
IC3	205 (14)	192 (94)	13 (06)	62 (38)	93 (57)	8 (05)	42
IC4	249 (18)	207 (83)	42 (17)	62 (31)	100 (51)	35 (18)	52
IC5	138 (10)	64 (46)	74 (54)	35 (34)	47 (46)	20 (20)	36
IC6	65 (05)	41 (63)	24 (37)	19 (38)	29 (58)	2 (04)	15
IC7	131 (09)	114 (87)	17 (13)	44 (40)	58 (52)	9 (08)	20
IC8	205 (14)	191 (93)	14 (07)	70 (46)	80 (53)	2 (01)	53
IC9	100 (07)	52 (52)	48 (48)	16 (22)	40 (54)	18 (24)	26
IC10	166 (12)	39 (23)	127 (77)	31 (26)	48 (40)	40 (34)	47

values are counts (percentage where present)

TABLE 2

CTL expression scores

	CTL score (all)	CTL score (*TP53*-WT)	CTL score (*TP53*-mutant)
ER-positive	−0.91	−0.07	0.01
ER-negative	0.31	0.58	0.16
Luminal A	−0.19	−0.16	−0.06
Luminal B	−0.18	−0.18	−0.02
Normal-like	0.25	0.29	0.27
HER2-enriched	0.16	0.34	0.04
Basal-like	0.42	0.88	0.20
IC1	−0.06	−0.05	0.15
IC2	−0.08	−0.07	0.05
IC3	−0.02	−0.01	0.21
IC4	0.39	0.43	0.35
IC5	0.08	0.18	−0.02
IC6	−0.24	−0.22	−0.17
IC7	−0.22	−0.20	−0.08
IC8	−0.41	−0.36	−0.34
IC9	−0.08	−0.07	0.02
IC10	0.28	0.76	0.15